Therapeutic Nano-Object Delivery to Sub-domains of Cardiac Myocytes

Valeriy Lukyanenko, Ph.D.

Medical Biotechnology Center, University of Maryland Biotechnology Institute, Baltimore, Maryland 21201

Correspondence to: Valeriy Lukyanenko, Ph.D.
Medical Biotechnology Center
University of Maryland Biotechnology Institute
725 W. Lombard St., Rm S216
Baltimore, MD 21201
Tel: (410) 706-8559, (410) 428-4599
Fax: (410) 706-8184
E-mail: lukyanen@umbi.umd.edu or
lukyanenko_home@yahoo.com

Content:

1. Introduction

Heart failure develops when the amount of blood pumped from the heart is inadequate to meet the metabolic demands of the body [1]. Heart failure is a syndrome with many different well-described causes, including myocardial infarction, pressure overload, volume overload, viral myocarditis, toxic cardiomyopathy and mutations in genes encoding for sarcomeric or cytoskeletal proteins [1]. At least half of the causes lead to relatively slow deterioration in heart functioning, during which some cells are more damaged then others. The creation of nanocarriers to deliver specific markers, drugs and therapeutic genes should make it possible to recognize sick cardiac cells and cure them individually. In other words, targeted delivery of analytic probes and therapeutic agents to cardiac myocytes and cellular compartments could significantly increase the efficiency of both diagnostic and treatment protocols for heart failure and have a significant impact on heart failure research.

On the way to their cardiac targets, nano-objects must penetrate multiple barriers including capillary walls, the sarcolemma, and intracellular barriers, which are unique to the structure of cardiac myocytes [2]. The size and coating of the carriers must allow them to reach the target and go through intracellular barriers. The particles have to be coated with a shell that includes compounds preventing aggregation and non specific binding of nano-objects, and specific molecules that (1) improve recognition of the target cell, (2) promote the binding to the cell membrane, (3) facilitate transportation through the cellular membrane, (4) defend the cargo compound from low lysosomal pH, and (5) have a “key” for entering the

intracellular structure.

For nanotechnology involved in the therapy of vascular problems resulting in heart failure please see the reviews by Kong & Goldschmidt-Clermont [3] and Brewster *et al.* [4].

2. Structure of ventricular cell

Cardiac myocytes are rod-shaped cells ~100 μm in length and 20-30 μm thick (Figure 1). The characteristic cardiac stripes seen with light microscopy are a combination of extracellular Z-grooves and cytoskeletal Z-lines (Figure 1*A*). The sarcolemma of ventricular cells (biggest cardiac myocytes) has multiple invaginations, called T-tubules, longitudinally connected to the transverse-axial tubular system (TATS) [5, 6]. Figure 1*B* shows a complicated network of the TATS tubules penetrating the entire thickness of the ventricular myocyte. Z-lines separate the myocytes into structurally similar sarcomeres. A longitudinal section presented in Figure 1*C* shows the main structures of the sarcomere: myofilaments, the myofibrillar and intermyofibrillar mitochondria, network and junctional SR, and transverse tubules (T-tubules) of the TATS.

Thus, the diffusion pathways for nano-objects inside a ventricular myocyte can be divided into two groups: (1) the tubules of the TATS, and (2) sarcoplasmic aqueous diffusion pathways [7]. The former is not a true intracellular system because of its multiple contacts with the extracellular space through T-tubules. The diameters of the TATS tubules usually fall within the range of 200 - 400 nm [6]. However, they are filled with the glycocalyx [6], so the real clearance of the

TATS pathway for nano-objects is ~10 nm [7]. Therefore, under normal conditions about 50% of the sarcolemma in cardiac ventricular myocytes is not available for transport of nano-objects >10 nm.

The ultrastructure of cardiac myocytes suggests the existence of intracellular barriers significantly restricting the diffusion of nano-objects towards functionally important cellular compartments and structures such as the nucleus, mitochondria, and the space between the junctional sarcoplasmic reticulum (jSR) and the T-tubules (so-called junctional cleft) (Figure 1*C*).

Figure 2*A* shows the primary targets and possible barriers and pathways for nano-objects within a cardiac myocyte. Targeting the nucleus and mitochondria is important because of their role in protein expression and cell energetics. The TATS sarcolemma contains numerous transporting structures and receptors crucial for cardiac function. The structural organization of the space around the jSR is a matter of special interest because of its direct involvement in excitation-contraction coupling [8]. Electron micrographs show how tightly the intracellular microstructures are packed in this peri-T-tubule region (Figure 1*C*) [7, 8]. Under pathological conditions cardiac cells undergo so-called ultrastructural remodeling which increases the distance between the structures and makes them available for nano-objects.

3. Nano-objects and their analytical applications

All nanostructures with important analytical applications could be divided into two groups: (1) nano-objects (nanotubes, spherical nanoparticles,

macromolecules, etc.) and (2) nanodevices (nanocapacitors, nanopores, nanocantilevers, etc.) [2]. Nano-objects can be used in a variety of bioanalytical formats [2]: (1) as quantitative tags, such as the optical detection of quantum dots and the electrochemical detection of metallic nanoparticles; (2) as substrates for multiplexed bioassays (encoded nanoparticles such as striped metallic nanoparticles); (3) as controllers of signal transduction (for example in colloidal gold-based aggregation assays); or (4) as catalyzers or inducers of biological processes (*i.e.* nonviral vectors). Chemotherapeutic and imaging nano-objects are usually conjugated to a chemotherapeutic drug (*i.e.* folic acid, paclitaxel, doxorubicin, *etc.*) and/or imaging agent (FITC, GFP, *etc.*).

Nano-objects that have been suggested for biomedical research have diameters from 0.8 to 400 nm [2, 9]. Note that the two most popular groups of viral vectors for gene transfer are 20 nm (adeno-associated virus), and 60-90 nm (adenovirus) in diameter [10]. Although all nano-objects within the 2–100 nm size range were found to alter signaling processes essential for basic cell functions, 40- and 50-nm nanoparticles demonstrated the greatest effect [11]. Nano-objects could be injected directly into the tissue, but a pumping heart is not a convenient target for an injection. Therefore, intravenous injection is the most appropriate way for delivery of nano-objects to the myocardium. Note that only nano-objects < 100 nm were shown to be optimal for intravenous injection [12, 13]. The pathway for nano-objects from the blood stream to the target intracellular sub-domain *in vivo* has three barriers: (1) vascular wall, (2) cell membrane (sarcolemma), and (3) intracellular barriers. Experiments with gold nanoparticles showed that they

have about 1 hour to pass the capillary endothelial barrier before being ingested by macrophages [14].

4. Cardiac vascular permeability

One of the most critical issues for successful nano-object delivery is the ability of the nano-objects to penetrate the vascular wall. The most vulnerable place for the penetration of the nano-objects from the blood into myocardium is a thin blood capillary wall. Penetration of nanoparticles also occurs in arterioles and venules, however in this case they are rapidly ingested by phagocytic elements located along the vessels [14].

The penetration of unsolved particles through the capillary wall depends on transcapillary filtration pressure (Starling forces) and permeability pathways [15, 16]. The capillary wall (Figure 2*B*) has three layers: internal tunic (endothelial cells), middle tunic (basement membrane), and adventitial tunic (cells and fibers). However, structural details of the capillaries are different for different tissues and could lack the internal tunic and/or adventitial tunics [14]. In the myocardium the blood capillaries are characterized by an extremely flat internal tunic (100-200 nm) and an irregular adventitial tunic. The middle tunic (20-50 nm) of the cardiac capillary wall consists mainly of collagenous and noncollagenous glycoproteins [14, 17]. Blood capillaries do not have a fenestrated endothelium encountered in many viscera, where the middle tunic is a major barrier between the vascular lumen and the interstitium [14]. In the cardiac capillary under normal conditions the primary barrier for nano-objects is the internal tunic, while the basement

membrane is not a barrier at least for particles that can penetrate the internal tunic [14, 18].

There are three pathways for nano-objects through the capillary endothelial barrier: passage between endothelial cells, transporting vesicles (caveolae), and transendothelial channels [14, 19]. The endothelial cells are tightly connected by tight, gap and adherens junctions [18, 20, 21]. The density of the junctions varies between organs, and they are maximally enriched in the brain (blood-brain barrier) where strict control of endothelial permeability is exerted between the blood and the central nervous system. In the heart the distance between endothelial cells is ~10 nm, and the gap is occupied by material of moderate density [14], which is probably junction structures and an overlay of two glycocalyxes (200-500 nm each [16, 18]). It was shown that the passage between endothelial cells is available only for objects <2 nm [19].

Nano-objects up to 50-70 nm in size could pass the endothelial barrier in the heart through membrane transporting vesicles, caveolae (the average diameter is ~ 70 nm), and transendothelial channels formed by the fused vesicles [14, 19, 20]. It is important to note for drug delivery purposes that caveolae vesicles do not contain any enzymatic cocktail and the cargo to be delivered by nano-objects would not be degradated by lysosomal enzymes [23].

Taking into account that the thickness of endothelial cells in a heart capillary could be only 100 nm [19], the transendothelial channel could be a primary pathway for 2-50-nm particles. In other words, theoretically under normal conditions the capillary barrier should be "transparent" for particles ≤50 nm.

However, practically, even 15-30-nm particles were not found in the heart after intravenous injections [24, 25]. So far, only the delivery of cerium oxide nanoparticles (average particle diameter 7 nm) to cardiac myocytes was confirmed after intravenous injection [26].

Transportation of 30-50-nm particles by the transporting vesicles could be significantly improved with coating by albumin and/or opening of additional pathways with specific agents [15, 19, 27, 28]. The passage between endothelial cells could be “unlocked” and also used for delivery of nano-objects. For instance, the opening of interendothelial junctions (up to 2 μm) in capillary and venular endothelium could be induced with nitric oxide synthase inhibitor L-NAME [28].

Under some pathological conditions the cardiac capillary barrier for nano-objects practically vanishes. For instance, hyperpermeability in the heart was shown to be triggered by inflammation or ischemia [20]. Also, during tissue inflammation the endothelial junctions were shown to widen (to 0.1-3 μm) in localized areas [18]. Acute inflammatory mediators, such as histamine and serotonin, significantly increase transportation of nano-objects by the vesicles and formation of transendothelial channels in cardiac endothelial cells [14]. Baldwin and Thurston (2001) showed that histamine destroyed the endothelial barrier within 10 minutes [18]. Thus, the inflammatory mediators could be used to improve the transcapillary transport of nano-objects.

The consequences of vascular permeability *in vivo* vary by location and depend on the situation. In the heart under normal physiological conditions the permeability response is tightly regulated and reversible. However, if platelets and

leukocytes are recruited to the site of the leak, the tissue damage could be irreversible [20].

5. Transmembrane pathways for internalization of nano-objects

Translocation of nano-objects across cell membranes depends on particle size, surface chemistry (coating), surface charge, and shape [2, 23]. There are four mechanisms for delivery of nano-objects through the cell membrane [2, 23, 29]: (1) clathrin-mediated endocytosis, (2) caveolae-mediated endocytosis, (3) macropinocytosis, and (4) nonspecific transport.

Clathrin-mediated endocytosis is a primary mechanism of internalization of nano-objects <200 nm [30]. It occurs in a membrane region enriched in clathrin. Formation of an endocytotic vacuole is driven by polymerization of clathrin units [23, 29]. Note that this transporting mechanism leads nano-objects to degradative lysosomes. Therefore clathrin-mediated endocytosis should be avoided for drug and gene delivery unless the cargo is protected or this is necessary (for instance, for target delivery of lipophilic agents, or disruption of endosomes through pH-sensitive mechanisms) [2, 23, 31, 32]. This transportation could be facilitated by the inclusion into the nano-object coating of virus coat proteins (*i.e.* TAT from HIV-1) or their analogs, or cell adhesion molecules (CAMs): integrins, cadherins, selectins, and immunoglobulins [31, 33, 34].

Caveolae-mediated endocytosis is predominant for nano-objects >200 nm [30]. Caveolae are membrane invaginations lined by caveolin [29]. They are abundant in cardiac myocytes [35]. Unlike clathrin-mediated endocytosis,

caveolae-mediated endocytosis is a highly regulated process, involving complex signaling [23]. Caveolae do not contain any enzymatic cocktail and could be employed as a primary transporting mechanism for drug and gene delivery with nano-objects. It was suggested that the switch between caveolae- and clathrin-mediated endocytosis could be made by pluronic P85 in a certain aggregation state: P85 unimers were shown to internalize through caveolae-mediated endocytosis, while P85 micelles internalize through clathrin-mediated endocytosis [36].

Macropinocytosis occurs via the formation of actin-driven membrane protrusions generating endocytic vesicles >1 μm in diameter [23, 29]. Macropinosomes do not have a specific coating. They can fuse with lysosomes and acidify. Macropinocytosis occurs in cardiac myocytes [37] and theoretically could be used for delivery of nano-objects up to 1000 nm in size.

Nonspecific transport of nano-objects includes (1) clathrin- and caveolae-independent endocytosis and (2) translocation that does not involve total enveloping of the nanoparticles by the membrane. The former involves cholesterol-rich microdomains, ‘rafts’, which are ~50 nm in diameter and diffuse freely on the cell surface [29]. The latter depends on their electrostatic interactions with charged membrane domains governing the adsorption of the nanoparticles onto the cell membrane [23, 38]. This mechanism of uptake was shown for nano-objects of 20-60 nm in size [39, 40]. However, the use of cationic coating for nano-objects is problematic in the case of intravenous injection due to interaction with negatively-charged serum proteins and red blood cells.

Thus, theoretically, for ventricular myocytes, there are four possible mechanisms for transport of nano-objects through the cell membrane. Although the mechanisms of nano-object transport through the sarcolemma of cardiac myocytes remain to be clarified, some morphological data suggest that it is similar to that described above. Two types of vesicles, coated and uncoated (~100 and ~50 nm correspondingly), that could be involved in transporting particles into cells have been demonstrated in cardiac myocytes [5, 41].

Due to the specific organization of ventricular myocytes, more than 50% of their sarcolemma belongs to T-tubules (Figure 1*B*). The tubules are filled with glycocalics and under normal conditions are available only for particles < 10 nm [7]. However, under some pathological conditions T-tubule dilation makes this sarcolemma opened for transportation of nano-objects.

Independently of the mechanism of internalization, disruption of the endosomal membrane must occur to release the nano-objects. In the case of clathrin-mediated endocytosis such disruption could be induced by pH-sensitive mechanisms (such as hydrazone linkers or DOPE [23]). Also, mechanisms of osmotic swelling to disrupt lysosomes, or pH buffering to protect the cargo could be employed [23, 38].

In the case of targeted gene delivery, it was found that, without the disruption of endosomes, at most only one plasmid out of 100 was effective [38]. However, even after a nano-object escapes the lysosome, its future could be questionable due to mechanical restrictions for diffusion. For example, it was shown that plasmid DNA (>20 nm in diameter) injected into the cytoplasm of rat

myotubes mostly remained at its site of the injection, probably being constrained by the actin cytoskeleton [38].

6. Intracellular barriers for nano-objects

Nano-objects can reach an intracellular target by passive diffusion or actively by utilizing the microtubule network (retrograde transport to the nucleus), as it has been shown for DNA [38]. Such an active microtubule-mediated cytosolic transport could probably also be employed for the delivery to the nuclear pore complex (NPC) of similarly sized nano-objects [23]. The incorporation of Fab fragments of antibodies against the molecular motor protein dynein into the nano-object coating should significantly facilitate this transportation [38]. Recently, the retrograde transport to the nucleus was shown to be enhanced with pluronics [42].

Free diffusion of nano-objects within cardiac myocytes has some restrictions [2, 7]. Moreover, some cellular subdomains such as mitochondrial intermembrane space, intermitochondrial contacts, mitochondria-junctional SR contacts, and junctional clefts are practically unavailable even to particles as small as 3 nm [2, 7, 43]. The 3-nm nano-objects diffuse freely to the nucleus and under some conditions can enter the mitochondrial intermembrane space (Figure 2C).

Nanoparticles >6 nm in size cannot diffuse into the nucleus or mitochondrial intermembrane space (Figure 2*D,E*) due to the clearance within the NPC (~5.5 nm) and porin (or VDAC; ~3 nm) [2]. Certain parts of “free” intracellular space within cardiac myocytes are relatively unavailable for nano-objects >3 nm [7]. For instance, Figure 2*E* shows that after silver enhancement 6-nm particles

can be found with much higher probability along Z-lines than along myofibrils.

The 3-nm clearance excludes passive diffusion of nanoparticles into mitochondrial intermembrane space. Moreover, the 3-nm objects probably cannot enter the mitochondrial matrix, the zone of highest interest for nanomedicine [43, 44]. Therefore, the use of the phenomenon of mitochondrial fusion was suggested for nanoparticle delivery [2, 23].

The most important target for contemporary bioresearch and therapy is the delivery of nano-objects to the nucleus. Cardiomyocytes do not undergo mitotic reorganization of the nuclear envelope, and for nano-objects the NPC is the only gate to the nucleus. There are two mechanisms of translocation across the NPC: passive diffusion and active transport. Although the NPC central channel has a limiting diameter of ~25–30 nm [38], it is known that molecules <60 kDa (<3.5 nm [45]) and nano-objects smaller than 5.5 nm can freely diffuse through the NPC due to a polymeric mesh in the pore [46-48].

Contemporary polymeric gene delivery systems are between 40 and 400 nm in size [9]. This mainly keeps them out of nucleus. So far only nano-objects <40 nm were shown to enter the nucleus [33]. Such transportation required the presence of a translocation signal (also known as a protein transduction domain or nuclear localization) in the coating of the nano-object to be recognized by the NPC transport receptors called karyopherins (importins α and β) and to form a nuclear pore targeting complex [38, 48]. There are many classes of signal localization sequences. Some of the signals (such as the peptide nuclear localization signal derived from the large T antigen of the SV40 virus, a peptide

derived from the HIV Tat protein, adenovirus fiber protein, and modified integrin binding domain peptide) were already shown to be helpful in the delivery of nano-objects to the nucleus [33, 49-52]. Active nuclear transport is regulated by many mechanisms (such as phosphorylation/dephosphorylation and protein cofactors [38, 48]) that have to be employed to facilitate the delivery of nano-objects to nucleus.

7. Changes in ventricular cell ultrastructure associated with heart failure

The symptoms of heart failure include hypertrophy [53], defined as an enlarged heart size and muscle mass during dilated (congestive) cardiomyopathy. On the ultrastructural level, heart hypertrophy is characterized by lobulated nuclei, multiple intercalated discs, dilated T-tubules, abnormal I bands, myofibrillar lysis, abnormally small mitochondria, and increased numbers of ribosomes [54-57]. Electron microscopy shows a significant reduction in the density of intermyofibrillar mitochondria and a reduction of mitochondrial number and size [2]. Dilated T-tubules should make available for anchoring of nano-objects some proteins that are preferentially located within the TATS (such as L-type calcium and brain-type Na^+ channels [58; 59]).

These heart failure-related changes have to result in significant changes in the pathways for targeted nano-objects delivery [2]: (1) dilated T-tubules approximately double the surface of the sarcolemma available for transport of nanoparticles and, consequently, the probability of delivery to failed cells, (2) diffusion pathways empty of glycogen and small mitochondria give more freedom

for nano-objects to diffuse within failing cells, (3) transformed mitochondria become much more available for nanoparticles. On the whole, even taking into account the slowing of physiological processes, the probability to deliver nano-object to a certain subdomain of a failing cell could be significantly higher than for a healthy myocyte.

8. Methods for studying the delivery of nano-objects to intracellular sub-domains of cardiac myocytes

Delivery of genes and drugs requires the creation of reliable delivery systems. The methods available for monitoring the delivery of nano-objects to intracellular sub-domains could be divided into visualization of nano-objects and retrieval of the products of the nano-object delivery. The latter is especially important in the case of gene delivery when the synthesis of certain proteins (or its inhibition) clearly confirms the delivery. This method, however, has some restrictions. Overexpression of any protein in cardiac myocytes can result in heart failure, probably due to obstruction of diffusion pathways [60]. Therefore, protein synthesis must be inhibited with doxycycline [61, 62]. This, however, reduces the synthesis of other cell proteins as well.

The former, visualization, clearly shows the location of nano-objects. Unfortunately, the popular method for intracellular and intraorganellar localization of nano-objects with confocal microscopy is significantly complicated in cardiac myocytes due to multiple membrane invaginations, low resolution of confocal systems, and out-of-focus light [63]. To avoid these problems we improved the

electron microscopy method developed by Feldherr [2, 7, 64]. The method employs electron microscopy, water-soluble resin for cell polymerization, and silver enhancement within ultrathin sections. This approach allows precise localization of 2-nm gold particles that could be tagged to any nano-object.

9. Confirmed deliveries of nano-object to cardiomyocytes *in vivo*

Dr. Torchilin's laboratory reported the successful delivery of DNA- or ATP-loaded immunoliposomes specific for cardiac myosin to cardiomyocytes of ischemic myocardium after intravenous injection [65, 66]. This significantly improved heart contractility after global ischemia. Dr. Kolattukudy's laboratory demonstrated cardioprotective effects of cerium oxide (CeO_2) nanoparticles in cardiomyopathy [26]. The nanoparticle treatment attenuated progressive cardiac dysfunction and remodeling in a murine model of ischemic cardiomyopathy. Authors attributed this beneficial effect of CeO_2 nanoparticles to their autoregenerative antioxidant properties inhibiting myocardial oxidative stress, ER stress and inflammatory processes.

Two groups reported successful cardiac transgene expression *in vivo* using an adeno-associated virus and cardio-selective promoters for intravenous injection. Although under these conditions all organs were shown to be infected, the promoters allow activation of delivered genes only in cardiomyocytes [67]. Dr. Koch's group targeted myocardial beta-adrenergic receptor signaling and calcium cycling with an adeno-associated virus [68]. They showed a stable myocardial-specific expression of a therapeutic transgene, the calcium Ca^{2+}-sensing S100A1,

which resulted in functional heart failure rescue in a rat model of heart failure [69].

Recently, Dr. Joseph Metzger's laboratory performed in vivo transgene expression of a cytosolic Ca^{2+} buffer parvalbumin and adult cardiac Troponin I isoform cTnI A164H [50, 70]. The former significantly accelerated relaxation of the heart without affecting cardiac morphology or systolic function [70]. The latter significantly improved systolic and diastolic cardiac function and mitigated reperfusion-associated ventricular arrhythmias [10, 50, 70].

10. Conclusion

To exert their therapeutic action, many pharmacological agents and large regulatory molecules (*i.e.* anti-apoptotic drugs, enzymes, siRNA, shRNA, *etc*.; Figure 2*A*) have to be delivered intracellularly. Precise delivery of different biologically active molecules to cellular sub-domains of failing cardiac myocytes can benefit the entire heart function. Although the delivery of nano-objects to sub-domains of a cardiac cell is complicated and many aspects of the delivery remain to be clarified, the contemporary state of the field is very promising.

References

[1] Hasenfuss, G., and B. Pieske, “Calcium cycling in congestive heart failure,” *J. Mol. Cell*. *Cardiol*., Vol. 34, 2002, pp. 951-969.

[2] Lukyanenko, V., “Delivery of nano-objects to functional sub-domains of healthy and failing ventricular myocytes,” *Nanomedicine*, Vol. 2, No. 6, 2007, pp.

831-846.

[3] Kong, D. F., and P. J. Goldschmidt-Clermont, “Tiny solutions for giant cardiac problems,” *Trends Cardiovasc. Med*., Vol. 15, 2005, pp. 207-211.

[4] Brewster, L. P., Brey, E. M., and H. P. Greisler, “Cardiovascular gene delivery: The good road is awaiting,” *Adv. Drug Deliv. Rev*., Vol. 58, No. 4, 2006, pp. 604-629.

[5] Fawcett, D. W., and N. S. McNutt, “The ultrastructure of the cat myocardium. I. Ventricular papillary muscle,” *J. Cell Biol*., Vol. 42, 1969, pp. 1-45.

[6] Forbes, M. S., and E. E. van Neil, “Membrane systems of guinea pig myocardium: ultrastructure and morphometric studies,” *Anatomical Record*., Vol. 222, 1988, pp. 362-379.

[7] Parfenov, A. S., et al., “Aqueous diffusion pathways as a part of the ventricular cell ultrastructure,” *Biophys. J*., Vol. 90, 2006, pp. 1107-1119.

[8] Lukyanenko, V., Chikando, A., and W. J. Lederer, “Mitochondria in cardiomyocyte Ca^{2+} signaling,” *Int. J. Biochem. Cell Biol*., Vol. 41, No. 8, 2009, pp. 1-15.

[9] Park, T. G., Jeong, J. H., and S. W. Kim, “Current status of polymeric gene delivery systems,” *Adv. Drug. Deliv. Rev*., Vol. 58, 2006, pp. 467-486.

[10] Davis, J., et al., “Designing heart performance by gene transfer,” *Physiol. Rev*., Vol. 88, No. 4, 2008, pp. 1567-651.

[11] Jiang, W., et al., “Nanoparticle-mediated cellular response is size-dependent,” *Nature Nanotechnol*., Vol. 3, No. 3, 2008, pp. 145-150.

[12] Gupta, A. K.., and M. Gupta, “Synthesis and surface engineering of iron oxide

nanoparticles for biomedical applications," *Biomaterials*, Vol. 26, 2005, pp. 3995-4021.

[13] Sebestyén, M. G., et al., "Mechanism of plasmid delivery by hydrodynamic tail vein injection. I. Hepatocyte uptake of various molecules," *J. Gene Med*., Vol. 8, No. 7, 2006, pp. 852-873.

[14] Palade, G. E., "Blood capillaries of the heart and other organs," Circulation, Vol. 24, 1961, pp. 368-388.

[15] Predescu, D., Vogel, S. M., and A. B.Malik, "Functional and morphological studies of protein transcytosis in continuous endothelia," *Am. J. Physiol. Lung Cell Mol. Physiol*., Vol. 287, No. 5, 2004, pp. L895-901.

[16] Weinbaum, S., et al., "The structure and function of the endothelial glycocalyx layer," *Annu. Rev. Biomed. Eng*., Vol. 9, 2007, pp. 121-67.

[17] Timpl, R., and M. Aumailley, "Biochemistry of basement membranes," *Adv. Nephrol. Necker Hosp*., Vol.18, 1989, pp. 59-76.

[18] Baldwin, A. L., and G. Thurston, "Mechanics of endothelial cell architecture and vascular permeability," *Crit. Rev. Biomed. Eng.*, Vol. 29, 2001, pp. 247-278.

[19] Predescu, S. A., Predescu, D. N., and G. E. Palade, "Plasmalemmal vesicles function as transcytotic carriers for small proteins in the continuous endothelium," *J. Physiol*., 272, 1997, pp. H937-949.

[20] Weis, S. M., "Vascular permeability in cardiovascular disease and cancer," *Curr. Opin. Hematol*., Vol. 15, No 3, 2008, pp. 243-249.

[21] Dejana, E., et al., "Organization and signaling of endothelial cell-to-cell junctions in various regions of the blood and lymphatic vascular trees," *Cell Tissue*

Res., Vol. 335, 2009, pp. 17-25.

[22] Frizzel, R. A., and G. Schultz, “Ion conductance of extracellular shunt pathway in rabbit ileum,” *J. Gen. Physiol*., Vol. 59, 1972, pp. 318-346.

[23] Hillaireaua, H., and P. Couvreur, “Nanocarriers’ entry into the cell: relevance to drug delivery,” *Cell. Molec. Life Sci*., Vol. 2009 (in press).

[24] Bibby, D. C., et al., “Pharmacokinetics and biodistribution of RGD-targeted doxorubicin-loaded nanoparticles in tumor-bearing mice,” *Int. J. Pharm*., Vol. 293, No. 2, 2005, pp. 281-290.

[25] Vancraeynest, D., et al., “Myocardial delivery of colloid nanoparticles using ultrasound-targeted microbubble destruction,” *Eur. Heart J*., Vol. 27, No. 2, 2006, 237-245.

[26] Niu, J., et al., “Cardioprotective effects of cerium oxide nanoparticles in a transgenic murine model of cardiomyopathy,” *Cardiovasc. Res*., Vol. 273, No. 3, 2007, pp. 549-559.

[27] Predescu, D., et al., “Transcytosis in the continuous endothelium of the myocardial microvasculature is inhibited by N-ethylmaleimide,” *Proc. Natl. Acad. Sci. U S A*., Vol. 91, 1994, pp. 3014-3018.

[28] Predescu, D., et al., “Constitutive eNOS-derived nitric oxide is a determinant of endothelial junctional integrity,” Am. J. Physiol. Lung Cell Mol. Physiol., Vol. 289, 2005, pp. L371-381.

[29] Conner, S. D., and S. L. Schmid, “Regulated portals of entry into the cell,” *Nature*, Vol. 422, 2003, pp. 37-44.

[30] Rejman, J., et al., “Size-dependent internalization of particles via the

pathways of clathrin- and caveolae-mediated endocytosis," *Biochem. J.*, Vol. 377, 2004, pp. 159-169.

[31] Torchilin, V.P., "Recent approaches to intracellular delivery of drugs and DNA and organelle targeting." *Annu. Rev. Biomed. Eng*., Vol.8, 2006, pp. 343-375.

[32] Nan, A., et al., "Water-soluble polymers for targeted drug delivery to human squamous carcinoma of head and neck," *J. Drug Target*., Vol. 13, 2005, pp. 189-197.

[33] Tkachenko, A. G., et al., "Cellular trajectories of peptide-modified gold particle complexes: comparison of nuclear localization signals and peptide transduction domains," *Bioconjug. Chem*., Vol. 15, No. 3, 2004, pp. 482-490.

[34] Dunehoo, A. L., et al., "Cell adhesion molecules for targeted drug delivery," *J. Pharm. Sci*., Vol. 95, No. 1, 2006, pp. 1856-1872.

[35] Lin, E., et al., "Distribution patterns of the Na^{+}-Ca^{2+} exchanger and caveolin-3 in developing rabbit cardiomyocytes," *Cell Calcium*, Vol. 45, 2009, pp. 369-383.

[36] Sahay, G., Batrakova, E. V., and A.V. Kabanov, "Different internalization pathways of polymeric micelles and unimers and their effects on vesicular transport," *Bioconjug. Chem*., Vol. 19, No. 10, 2008, pp. 2023-2029.

[37] Donaldson, J. G., Porat-Shliom, N., and L. A. Cohen, "Clathrin-independent endocytosis: a unique platform for cell signaling and PM remodeling," *Cell. Signal.*, Vol. 21, No. 1, 2009, pp. 1-6.

[38] Miller, A. M., and D. A. Dean, "Tissue-specific and transcription factor-mediated nuclear entry of DNA," *Adv. Drug Deliv. Rev*., Vol. 60, 2009, (in press).

[39] Wilhelm, C., et al., "Intracellular uptake of anionic superparamagnetic

nanoparticles as a function of their surface coating," *Biomaterials*, Vol. 24, No. 6, 2003, pp. 1001-1011.

[40] Pitard, B., et al., "Negatively charged self-assembling DNA/poloxamine nanospheres for in vivo gene transfer," *Nucleic Acids Research*, Vol. 32, No. 20, 2004, pp. e159-167.

[41] McNutt, N. S., and D. W. Fawcett, "The ultrastructure of the cat myocardium. II. Atrial muscle," *J. Cell Biol*., Vol. 42, 1969, pp. 46-67.

[42] Yang, Z., et al., "Amphiphilic block copolymers enhance cellular uptake and nuclear entry of polyplex-delivered DNA," *Bioconjug. Chem*., Vol. 19, 2008, pp. 1987-1994.

[43] Salnikov, V., et al., "Probing the outer mitochondrial membrane in cardiac mitochondria with nanoparticles," *Biophys. J*., Vol. 92, 2007, pp. 1058-1071.

[44] Weissig, V., et al., "Mitochondria-specific nanotechnology," *Nanomedicine*, Vol. 2, 2007, pp. 275-285.

[45] Vandegriff, K. D., et al., "Colloid osmotic properties of modified hemoglobins: chemically cross-linked versus polyethylene glycol surface-conjugated," *Biophys. Chem*., Vol. 69, 1997, pp. 23-30.

[46] Bustamante, J.O., et al.,"Dendrimer-assisted patch-clamp sizing of nuclear pores," *Pflugers Arch*., Vol. 439, No. 6, 2000, pp. 829-837.

[47] Elbaum, M., "Materials science. Polymers in the pore," *Science*, Vol. 314, 2006, pp. 766–767.

[48] Faustino, R. S., et al., "Nuclear transport: target for therapy," *Clin. Pharmacol. Ther*., Vol. 81, 2007, pp. 880-886.

[49] Pusl, T., et al., “Epidermal growth factor-mediated activation of the ETS domain transcription factor Elk-1 requires nuclear calcium,” *J. Biol. Chem*., Vol. 277, 2002, pp. 27517-27527.

[50] Day, S. M., et al., “Histidine button engineered into cardiac troponin I protects the ischemic and failing heart,” *Nature Med.*, Vol. 12, 2006, pp. 181-189.

[51] Ryan, J. A., et al., “Cellular uptake of gold nanoparticles passivated with BSA-SV40 large T antigen conjugates,” *Anal. Chem*., Vol. 79, 2007, pp. 9150-9159.

[52] Guatimosim, S., et al., “Ca^{2+} regulates cardiomyocyte function,” *Cell Calcium*, Vol. 44, No. 2, 2008, pp. 230-242.

[53] Tomaselli, G. F., and D. P. Zipes, “What causes sudden death in heart failure?” *Circ. Res*., Vol. 95, 2004, pp. 754-763.

[54] Deshaies, Y., Willemot, J., and J. Leblanc, “Protein synthesis, amino acid uptake, and pools during isoproterenol-induced hypertrophy of the rat heart and tibialis muscle,” *Can. J. Physiol. Pharmacol*., Vol. 59, 1981, pp. 113–121.

[55] Jones, M., et al., “Ultrastructure of crista supraventricularis muscle in patients with congenital heart diseases associated with right ventricular outflow tract obstruction,” *Circulation*, Vol. 51, 1975, pp. 39-67.

[56] Su, X., Sekiguchi, M., and M. Endo, “An ultrastructural study of cardiac myocytes in postmyocardial infarction ventricular aneurysm representative of chronic ischemic myocardium using semiquantitative and quantitative assessment,” *Cardiovasc. Pathol*., Vol. 9, 2000, pp. 1-8.

[57] He, J., et al., “Reduction in density of transverse tubules and L-type Ca^{2+} channels in canine tachycardia-induced heart failure. *Cardiovasc. Res*., Vol. 49,

No. 2, 2001, pp. 298-307.

[58] Gu, Y., et al., " High-resolution scanning patch-clamp: new insights into cell function," *FASEB J*., Vol. 16, 2002, pp. 748-750.

[59] Maier, S.K., et al., "Distinct subcellular localization of different sodium channel alpha and beta subunits in single ventricular myocytes from mouse heart," *Circulation*, Vol. 109, 2004, pp. 1421-1427.

[60] Huang, W.Y., et al., "Transgenic expression of green fluorescence protein can cause dilated cardiomyopathy," *Nature Med*., Vol. 6, 2000, pp. 482-483.

[61] Tallini, Y. N., et al., "Imaging cellular signals in the heart in vivo: Cardiac expression of the high-signal Ca^{2+} indicator GCaMP2," *Proc. Natl. Acad. Sci. U S A*, Vol. 103, 2006, pp. 4753-4758.

[62] Kotlikoff, M. I., "Genetically encoded Ca^{2+} indicators: using genetics and molecular design to understand complex physiology," *J. Physiol*., Vol. 578, 2007, pp. 55-67.

[63] Pratusevich, V. R., and C. W. Balke, "Factors shaping the confocal image of the calcium spark in cardiac muscle cells," *Biophys. J.*, Vol. 71, 1996, pp. 2942-2957.

[64] Feldherr, C. M., and J. M. Marshall, "The use of colloidal gold for studies of intracellular exchanges in the ameba *Chaos chaos*," *J. Cell Biol*., Vol. 12, 1962, pp. 640-645.

[65] Verma, D. D., et al., "ATP-loaded immunoliposomes specific for cardiac myosin provide improved protection of the mechanical functions of myocardium from global ischemia in an isolated rat heart model," *J. Drug Target*, Vol. 14, No.

5, 2006, pp. 273-280.

[66] Ko, Y. T., et al., “Gene delivery into ischemic myocardium by double-targeted lipoplexes with anti-myosin antibody and TAT peptide,” *Gene Ther*., Vol. 16, No. 1, 2009, pp. 52-59.

[67] Pleger, S. T., Most, P., and W. J. Koch, “Recent findings into the potential of gene therapy to reverse heart failure,” *Expert. Opin. Biol. Ther*., Vol. 7, No. 12, 2007c, pp. 1781-1784.

[68] Pleger, S. T., et al., “Targeting myocardial beta-adrenergic receptor signaling and calcium cycling for heart failure gene therapy,” *J. Card. Fail*. Vol. 13, 2007a, pp. 401-414.

[69] Pleger, S. T., et al., Stable myocardial-specific AAV6-S100A1 gene therapy results in chronic functional heart failure rescue. *Circulation*, Vol. 115, 2007b, pp. 2506-2515.

[70] Day, S. M., et al., “Cardiac-directed parvalbumin transgene expression in mice shows marked heart rate dependence of delayed Ca^{2+} buffering action,” *Physiol. Genomics*., Vol. 33, No. 3, 2008, pp. 312-322.

Legends

Figure 1. Cardiac myocyte. (Reproduced from Nanomedicine (2007) 2(6), 831-846 [2] with permission of Future Medicine Ltd). (**A**) Image of a ventricular cell in transmitted light. (**B**) 3-D confocal imaging of transverse-axial tubular system (TATS). Optical cut through the center of the cell. The TATS tubules are marked

with di-8-ANEPPS. (**C**) Electron micrograph; longitudinal ultrathin section. © 2006 Biophysical Journal [7]. Oblique section shows the localization of junctional SR (*jSR*) in relation to T-tubules and mitochondria (*M*). *MF*: myofilaments; *T*: T-tubule of TATS, *Z*: Z line.

Figure 2. Nano-objects and barriers for their delivery to subdomains of cardiac myocytes. (**A**) Nano-objects and their cardiac intracellular targets. Simplified schematic representation of intracellular targets for nano-objects in ventricular cell. (Reproduced from Nanomedicine (2007) 2(6), 831-846 [2] with permission of Future Medicine Ltd).*JC*: JUNCTIONAL CLEFT; *mDNA*: mitochondrial DNA; *siRNA*: synthetic small interfering RNA. (**B**) The capillary wall in the heart. © 2006 Biophysical Journal [7]. Diagram schematically represents three mechanisms of cardiac vascular permeability: (1) transport by plasmalemmal vesicles, (2) transendothelial channel made by the fused vesicles, and (3) intercellular space. (**C--E**) Distribution of gold nanoparticles in permeabilized ventricular myocytes. Representative electron micrographs show the distribution of 3- (**C**) and 6-nm (**D,E**) particles within ventricular cells. *M*: mitochondrion; *N*: nucleus; *Z*: Z line; *TT*: T-tubule. Ovals mark particles located deeper in the section and found with digitally enhanced contrast.

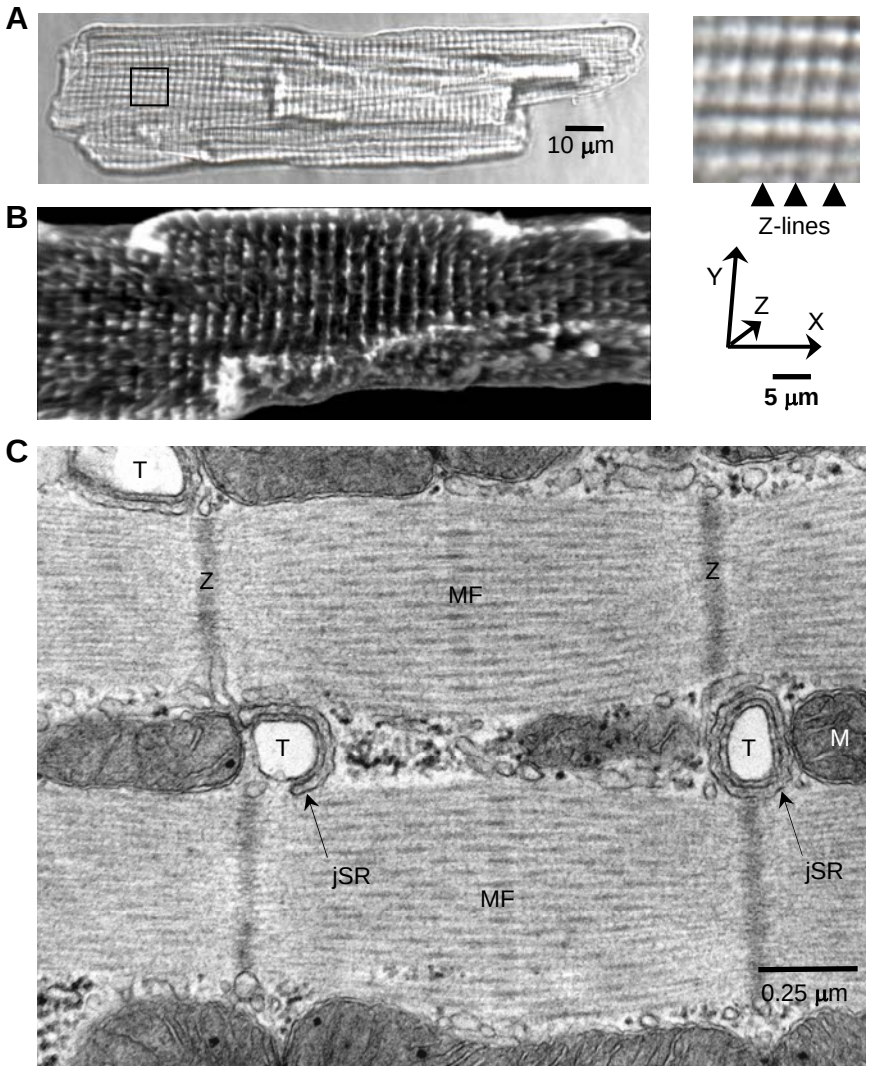

Figure 1

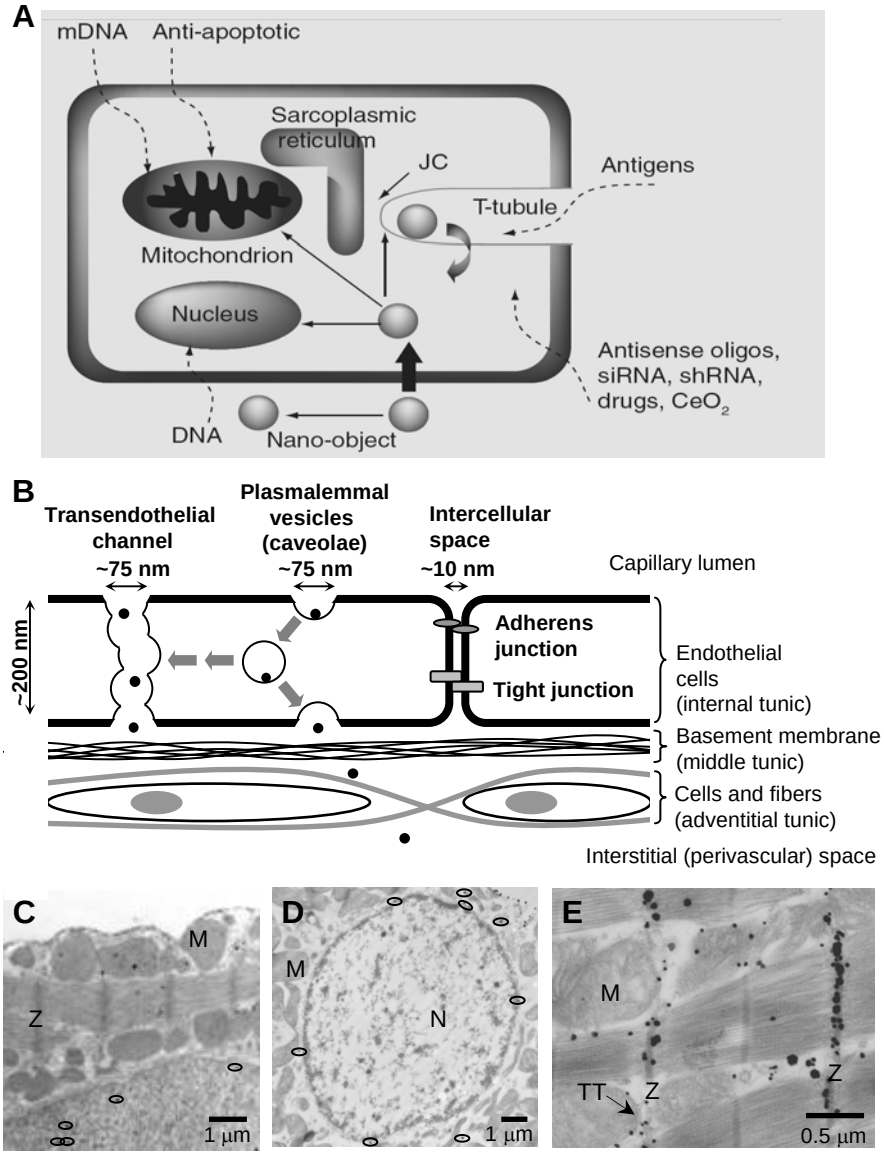
A
mDNA
Anti-apoptotic
Sarcoplasmic reticulum
JC
Antigens
T-tubule
Mitochondrion
Nucleus
Antisense oligos, siRNA, shRNA, drugs, CeO2
DNA
Nano-object
B
Transendothelial channel ~75 nm
Plasmalemmal vesicles (caveolae) ~75 nm
Intercellular space ~10 nm
Capillary lumen
~200 nm
Adherens junction
Tight junction
Endothelial cells (internal tunic)
Basement membrane (middle tunic)
Cells and fibers (adventitial tunic)
Interstitial (perivascular) space
C
M
Z
1 μm
D
M
N
1 μm
E
M
TT
Z
Z
0.5 μm

Figure 2